ICE ACCRETION PREDICTION ON AN ENGINE INLET

Serkan Özgen [1] , Nermin Uğur [1], İlhan Görgülü [2], Volkan Tatar [2]

1 Middle East Technical University, Department of Aerospace Engineering
2 TUSAŞ Engine Industries Inc.

Outline

- Motivation
- Methodology
- Results
- Conclusions
- Acknowledgement
- References

Motivation

- In-flight icing on airframes and engines may cause great risk to flight safety due to **aerodynamic performance degradation and engine performance losses.**
- It is very important to simulate ice accretion to develop **ice protection systems** and to comply with **Airworthiness Requirements** (FAR/CS-25, App. C and very recently, App. O and P).
- A computational tool is developed for icing analyses in FORTRAN language within the scope of SANTEZ 0046.STZ.2013-1 Project.
- With this tool, **collection efficiencies** and **ice shape predictions** for a nacelle geometry are obtained in the present study. The results are compared with experimental and numerical data presented by Bidwell and Mohler [1], Iuliano et al [2].

Methodology

Ice Accretion Modeling Modules

1. Flow field solution
2. Droplet trajectories and collection efficiency calculations
3. Thermodynamic analyses
4. Ice accretion calculation

Methodology

1. Flow field solution

Hess-Smith Panel method

- The velocity and pressure distribution on the surface for boundary layer calculations
- Off-body velocities for droplet trajectory calculations

Methodology

1. Flow field solution

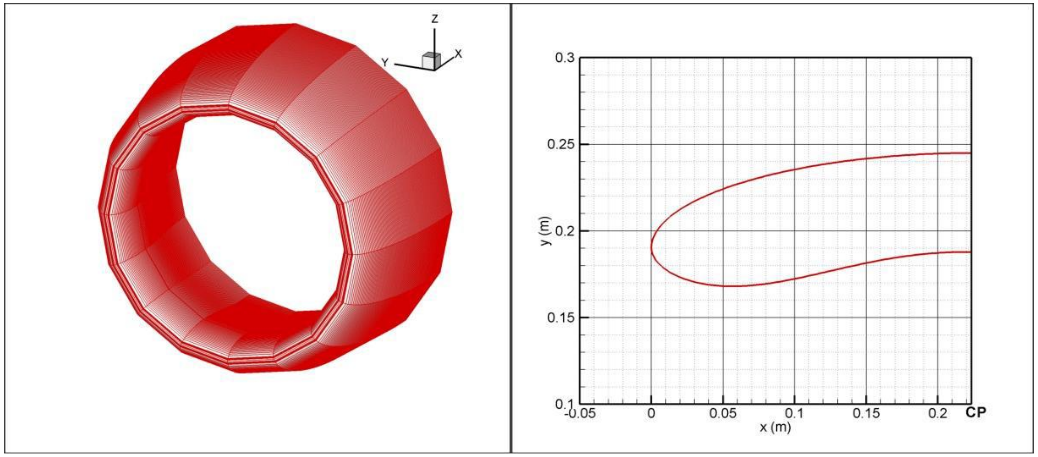

Figure 1: *Intake geometry*

- Outer and the inner cowls are defined by a super ellipse and an ellipse, respectively [2] .
- Length of the inlet: 0.2234 m
- Height of the inlet: 0.1905 m

Methodology

1. Flow field solution

Complicated to maintain both:

- the required flight conditions (freestream velocity)
- the desired mass flow rate through the intake

Superposition approach utilized by Waung [5]

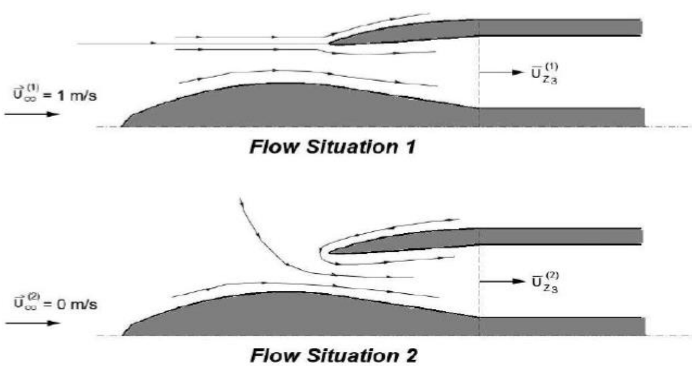

Figure 2: *Visual representation of two flow situations used in the superposition method [5]*

<u>Flow situation 1:</u> → N+1 unknowns
U_∞= 1 m/s, α=0º

<u>Flow situation 2:</u> → N unknowns
U_∞ =0 m/s, Γ = 1
(Γ:vortex strength along the surface panels)

➢ The final flow is obtained by scaling and combining these two solutions.

$$c_1 U_{\infty 1} + c_2 U_{\infty 2} = U_\infty \,,$$
$$c_1 \bar{U}_{cp1} + c_2 \bar{U}_{cp2} = \bar{U}_{cp} \,.$$

$$\boxed{c_1 = U_\infty \text{ and } c_2 = (\bar{U}_{cp} - U_\infty \bar{U}_{cp1})/\bar{U}_{cp2}.}$$

The velocity components are corrected for compressibility effects using the Prandtl-Glauert compressibility correction:

$$\hat{u} = \bar{u}/\sqrt{1-M^2}\,, \qquad \hat{v} = \bar{v}/\sqrt{1-M^2},$$

Methodology

1. Flow field solution

V_∞ (m/s)	α (degree)
75	0

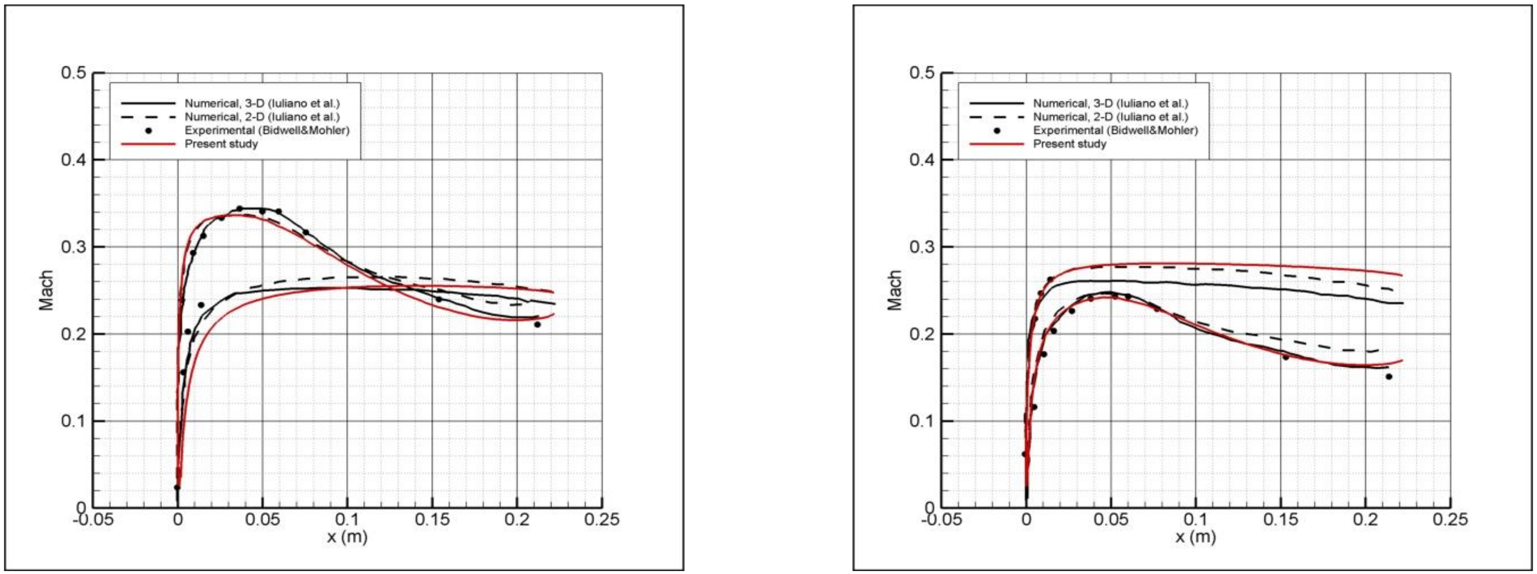

$a)\ \dot{\mathrm{m}} = 10.42\ \mathrm{kg/s}$ $b)\ \dot{\mathrm{m}} = 7.8\ \mathrm{kg/s}$

Figure 3: *Mach number distributions on the intake.*

Methodology

2. Calculation of droplet trajectories

Lagrangian approach

$$m\ddot{x}_p = -D\cos\gamma,$$

$$m\ddot{y}_p = -D\cos\gamma + mg,$$

$$\gamma = \tan^{-1}\frac{\dot{y}_p - V_y}{\dot{x}_p - V_x},$$

$$D = \frac{1}{2}\rho V_{rel}^2 C_D A_p,$$

$$V_{rel} = \sqrt{(\dot{x}_p - V_x)^2 + (\dot{y}_p - V_y)^2}.$$

Collection efficiency (β)

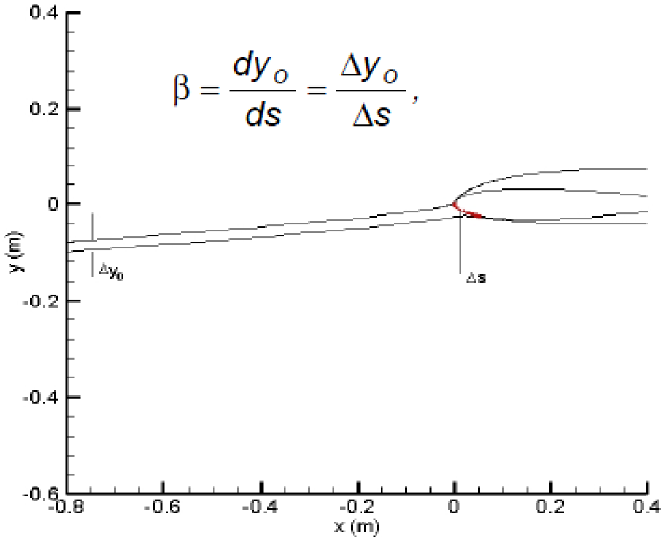

Figure 4: *Definition of collection efficiency*

Methodology

2. Calculation of droplet trajectories

$\dot{m}$ $\left({}^{kg}/_{s}\right)$	α (degree)
10.42	0

Collection efficiency results 1

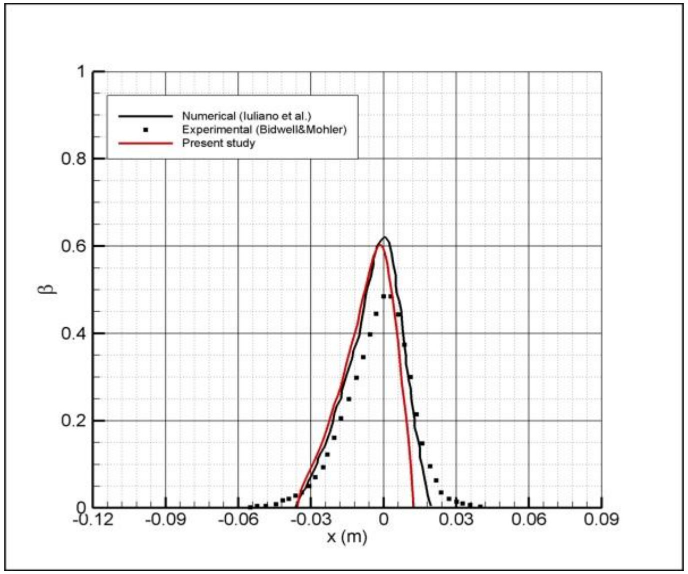

a) $d_p = 16.45\ microns$

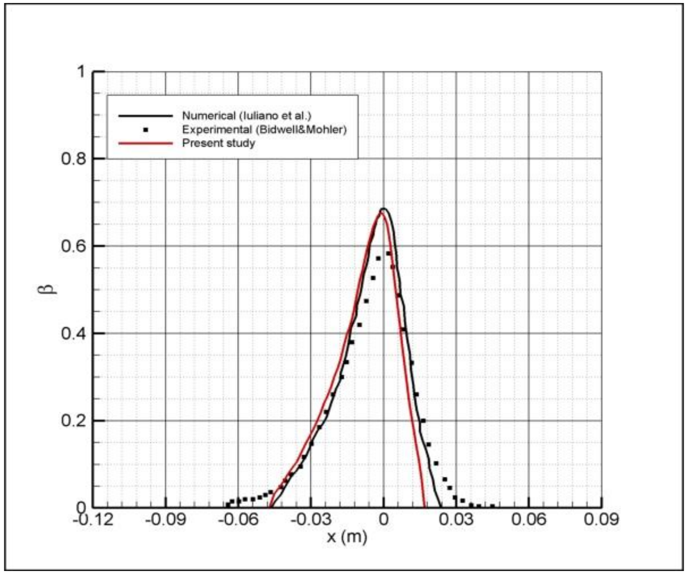

b) $d_p = 20.36\ microns$

Figure 5: *Collection efficiency distribution on the nacelle*

Methodology

$\dot{m}$ $({}^{kg}/{}_{s})$	α (degree)
7.8	0

2. Calculation of droplet trajectories

Collection efficiency results 2

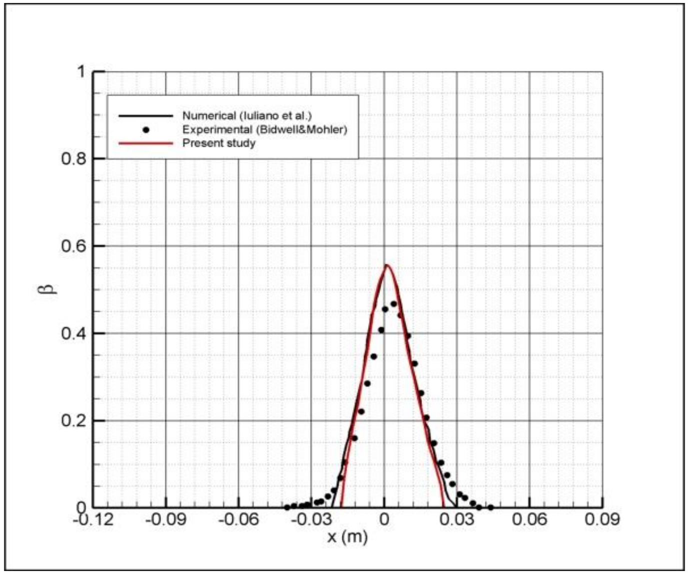

a) $d_p = 16.45\ microns$

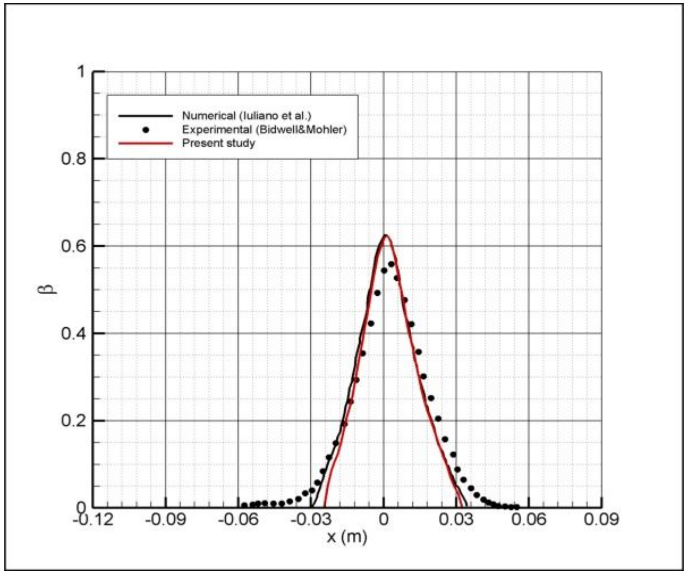

b) $d_p = 20.36\ microns$

Figure 6: *Collection efficiency distribution on the nacelle*

Methodology

3. Thermodynamic analyses

Calculation of convective heat transfer coefficients:

➢2D Integral Boundary Layer Method

Laminar

➢Smith and Spaulding

Turbulent

➢Kays and Crawford

▪Transition from laminar to turbulent flow occurs when the Reynolds number based on roughness height exceeds Re_k=600

where $$Re_k = \rho U_k k_s / \mu$$

Methodology

3. Thermodynamic analyses

V_∞ (m/s)	α (degree)
75	0

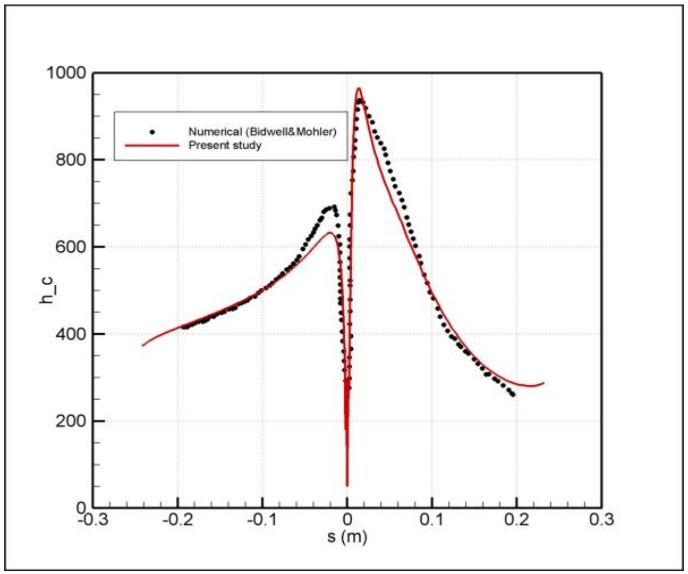

$\dot{m} = 10.42\ kg/s$

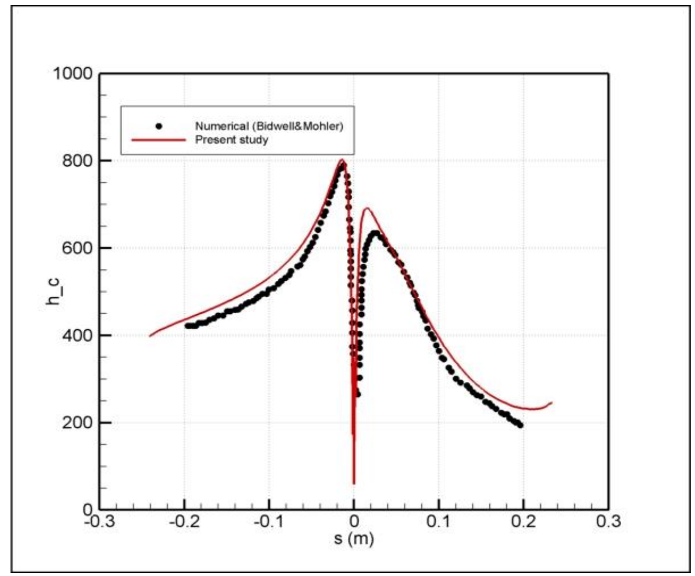

$\dot{m} = 7.8\ kg/s$

Figure 7: *The heat transfer coefficient distribution on the nacelle*

Methodology

4. Ice accretion calculation

- Extended Messinger Model [3]

<u>Stefan problem</u>

Energy equation for ice layer: $$\frac{\partial T}{\partial t} = \frac{k_i}{\rho_i C_{pi}} \frac{\partial^2 T}{\partial y^2} \ ,$$

Energy equation for water layer: $$\frac{\partial \theta}{\partial t} = \frac{k_w}{\rho_w C_{pw}} \frac{\partial^2 \theta}{\partial y^2} \ ,$$

Mass balance: $$\rho_i \frac{\partial B}{\partial t} + \rho_w \frac{\partial h}{\partial t} = \rho_a \beta V_\infty + \dot{m}_{in} - \dot{m}_{e,s} \ ,$$

Phase change condition: $$\rho_i L_F \frac{\partial B}{\partial t} = k_i \frac{\partial T}{\partial y} - k_w \frac{\partial \theta}{\partial y} \ ,$$

Methodology

4. Ice accretion calculation

Boundary and initial conditions for Stefan problem:

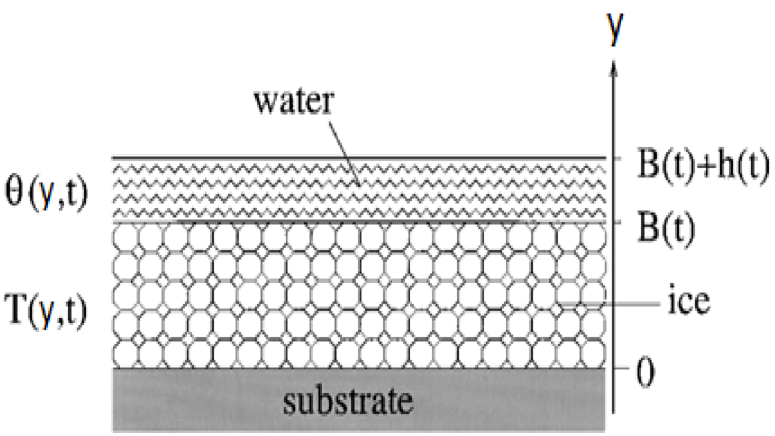

Figure 8: Water and ice layers on a surface [3]

1. $T(0,t)=T_s=T_a$
2. $T(B,t)=\theta\ (B,t)=T_f$
3. $B=h=0$ at $t=0$
4. At the air/water (glaze ice) or air/ice (rime ice) interface, heat flux is determined by convection (Q_c), radiation(Q_r), latent heat release(Q_l), cooling by incoming droplets (Q_d), heat brought in by runback water (Q_{in}), evaporation (Q_e) or sublimation (Q_s), aerodynamic heating (Q_a) and kinetic energy of incoming droplets (Q_k).

Methodology

4. Ice accretion calculation

- Rime ice growth : $$B(t) = \frac{\rho_a \beta V_\infty}{\rho_r} t$$
  (Algebraic equation)

- Glaze ice growth : $$\rho_g L_F \frac{\partial B}{\partial t} = \frac{k_i (T_f - T_s)}{B} + k_w \frac{(Q_c + Q_e + Q_d + Q_r) - (Q_a + Q_k)}{k_w}$$
  (1st order ODE)

- The equations are integrated over time using a variable stepsize Runge-Kutta integrator.

Results

Ice shape predictions

Table 1: *Icing conditions (V_∞=75 m/s, α=0º, t_{exp}=30 min)*

Case #	$\dot{m}\ (kg/s)$	$d_p\ (microns)$	$\rho_a\ (g/m^3)$	T_a (ºC)	Condition
1	10.42	16.45	0.2	-29.9	Rime
2	10.42	20.36	0.2	-29.9	Rime
3	7.8	16.45	0.2	-29.9	Rime
4	7.8	20.36	0.2	-29.9	Rime
5	10.42	16.45	0.695	-9.3	Glaze
6	10.42	20.36	0.695	-9.3	Glaze
7	7.8	16.45	0.695	-9.3	Glaze
8	7.8	20.36	0.695	-9.3	Glaze

Results

Rime ice condition 1

$\dot{m}$ (kg/s)	ρ_a (g/m^3)	T_a (°C)
10.42	0.2	-29.9

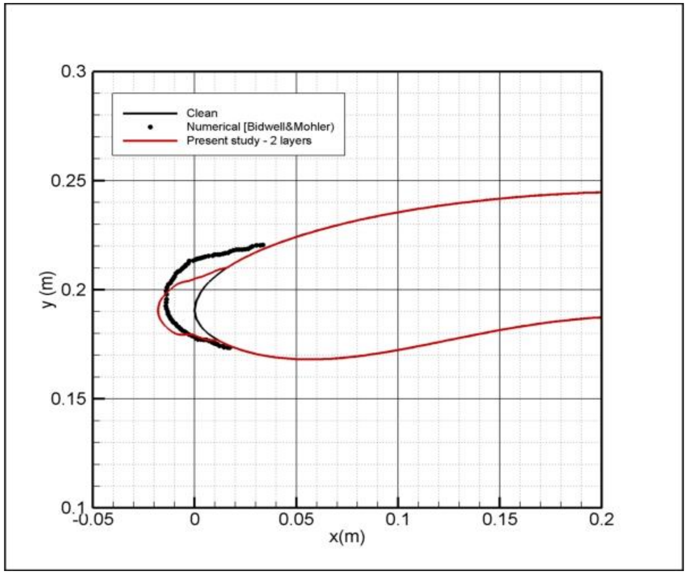

a) $d_p = 16.45\ microns$

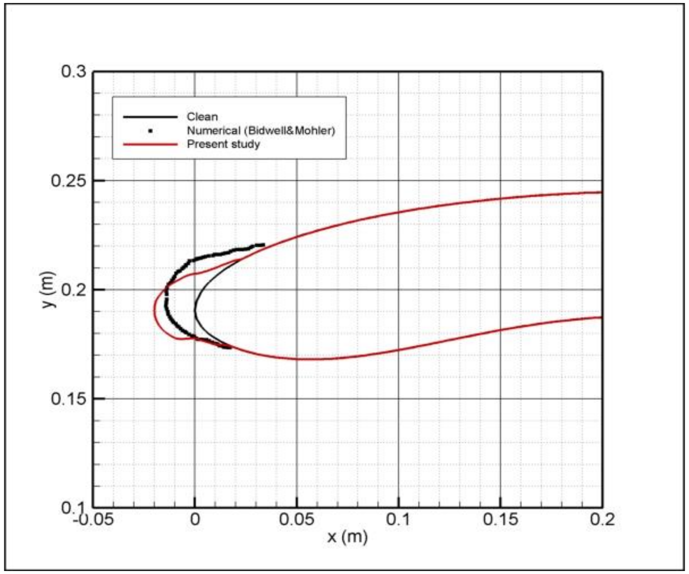

b) $d_p = 20.36\ microns$

Figure 9: *Ice shapes on the air intake*

Results

Rime ice condition 2

$\dot{m}\ (kg/s)$	$\rho_a\ (g/m^3)$	T_a (°C)
7.8	0.2	-29.9

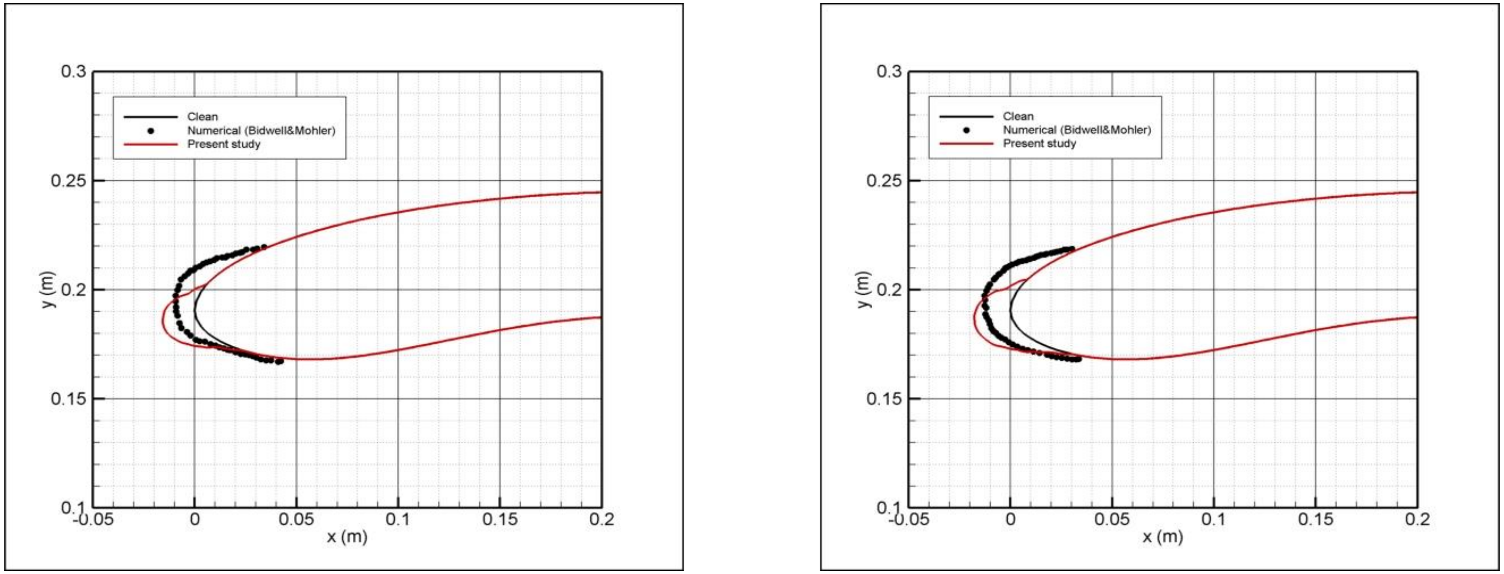

a) $d_p = 16.45\ microns$ b) $d_p = 20.36\ microns$

Figure 10: *Ice shapes on the air intake*

Results

Glaze ice condition 1

$\dot{m}\ (kg/s)$	$\rho_a\ (g/m^3)$	T_a (ºC)
10.42	0.695	-9.3

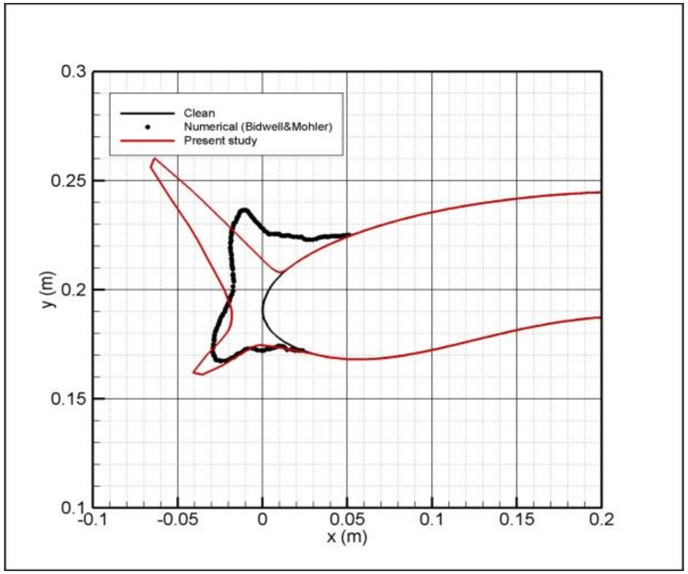

a) $d_p = 16.45\ microns$

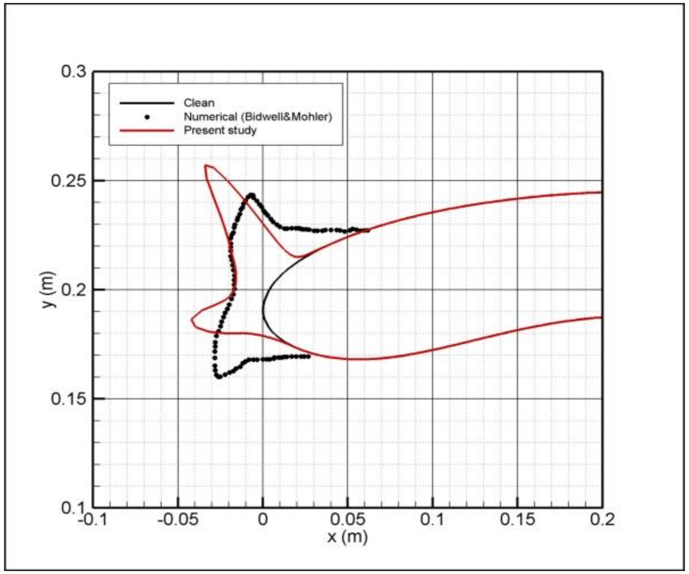

b) $d_p = 20.36\ microns$

Figure 11: *Ice shapes on the air intake*

Results

Glaze ice condition 2

$\dot{m}\ (kg/s)$	$\rho_a\ (g/m^3)$	T_a (ºC)
7.8	0.695	-9.3

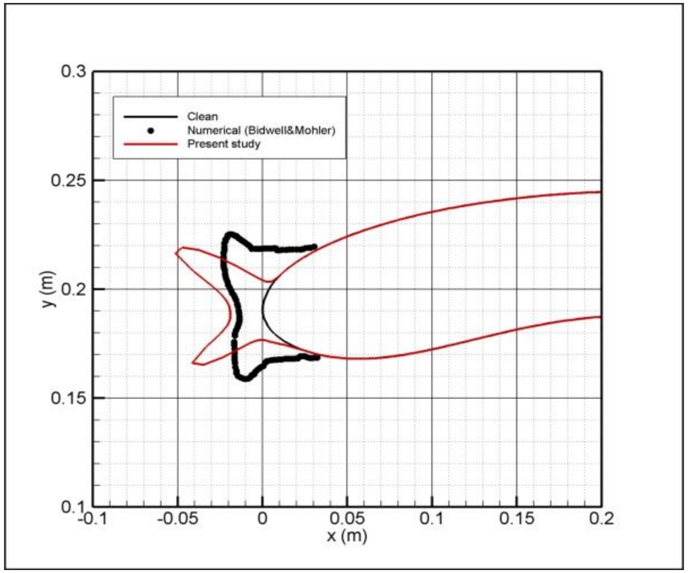

a) $d_p = 16.45\ microns$

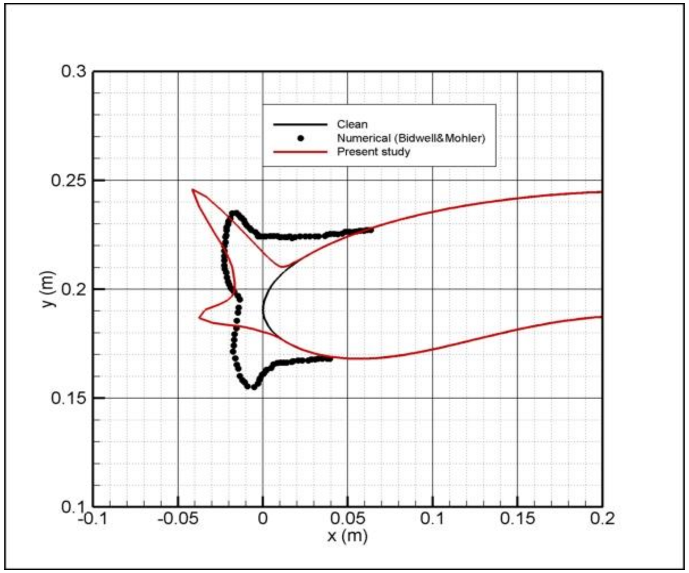

b) $d_p = 20.36\ microns$

Figure 12: *Ice shapes on the air intake*

Conclusions

- Collection efficiency and ice shape results are presented for a benchmark intake geometry in symmetrical flow conditions.
- It is concluded that larger droplets results in wider impingement zones and higher collection efficiencies.
- In other words, larger droplets lead to larger and thicker ice formations.
- It is also verified that the proposed method for maintaining the mass flow rate through the inlet is valid.

Acknowledgement

- Ministry of Science, Industry and Technology.

- TUSAŞ Engine Industries Inc.

References

[1] Bidwell, C.S. and Mohler, S.R. Jr., *Collection Efficiency and Ice Accretion Calculations for a Sphere, a Swept MS(1)-317 Wing, a swept NACA 0012 Wing Tip, an Axisymmetric Inlet and a Boeing 737-300 Inlet*, AIAA 95-0755, 1995. .

[2] Iuliano, E., Mingione, G., de Domenico, F. and de Nicola, C., *An Eulerian Approach to Three-Dimensional Droplet Impingement Simulation in Icing Environment,* AIAA Guidance, Navigation and Control Conference, Toronto, AIAA 2010-7077, 2010.

[3] Myers, T.G., Extension to the Messinger Model for aircraft icing, *AIAA J., Vol. 39, pp. 211-218, 2001.*

[4] Özgen, S., and Canıbek, M., Ice accretion simulation on multi-element airfoils using extended Messinger model, *Heat and Mass Transfer, Vol. 45 (3), pp. 305-322, 2009.*

[5] Waung, T.S., An Ejector Inlet Design Method for a Novel Rocket-Based Combined_cycle Rocket Nozzle, M.Sc. Thesis, Ottawa-Carlton Institute for Mechanical and Aerospace Engineering, 2010.